A study of the electron transfer and photothermal effect of gold nanorods on a glucose biosensor

2010 Nanotechnology 21 185504

(http://iopscience.iop.org/0957-4484/21/18/185504)

Nanotechnology **21** (2010) 185504 (6pp) doi:10.1088/0957-4484/21/18/185504

A study of the electron transfer and photothermal effect of gold nanorods on a glucose biosensor

Huiyu Liu[1], **Dong Chen**[2], **Liuqing Yang**[1,3], **Xiangling Ren**[1], **Fangqiong Tang**[1] **and Jun Ren**[1]

[1] Technical Institute of Physics and Chemistry, Chinese Academy of Sciences, Beijing 100190, People's Republic of China
[2] Beijing Creative Nanophase Hi-Tech Company, Limited, Beijing 100086, People's Republic of China
[3] Graduate School of the Chinese Academy of Sciences, Beijing 100049, People's Republic of China

E-mail: tangfq@mail.ipc.ac.cn

Received 9 February 2010, in final form 22 March 2010
Published 14 April 2010
Online at stacks.iop.org/Nano/21/185504

Abstract
A new glucose biosensor based on the electron transfer and photothermal effect of gold nanorods (GNRs) is reported here. The biosensor was prepared by immobilizing glucose oxidase (GO*x*) on a platinum (Pt) electrode by a composite film consisting of GNRs, polyvinyl butyral (PVB) and glutaraldehyde. GNRs were synthesized by a gold seed-mediated cetyltrimethylammonium bromide (CTAB) surfactant-assisted approach. The fabrication, characterization and analytical performance of the glucose biosensor based on GNRs are described in this paper. Moreover, the modulation of the biosensor by the photothermal effect based on the unique surface plasma resonance (SPR) property of GNRs was investigated for the first time. The results show that the current response of a glucose biosensor can significantly increase, induced by the electrical conductivity and photothermal effect of GNRs.

(Some figures in this article are in colour only in the electronic version)

1. Introduction

Biosensors have aroused much interest because of the advantage of carrying out analytical and diagnostic procedures simply and rapidly. Among various biosensors, a glucose biosensor has been considered to be important due to its potential ability to analyse glucose *in situ* in real time, which is essential to the appropriate administration of insulin in clinical diabetes therapy [1–3]. The most common strategy with glucose biosensors is the utilization of glucose oxidase (GO*x*) to produce hydrogen peroxide (H_2O_2) from glucose and then detect the glucose concentration by a change in current flow between hydrogen peroxide and an amperometric electrode [4]. However, since the active center of GO*x* is deeply buried in a protein shell, which forms a barrier to efficient electrical communication between the redox center of GO*x* and solid electrode surfaces [5], it is necessary to find a viable way to further enhance the efficiency of electrical communication.

In the past few years there has been growing interest in utilizing various nanoparticles, such as Ag [6], Fe_3O_4 [7], Pt [8], semiconductor nanoparticles (CdSe/ZnS) [9] and so on [10, 11], to immobilize the GO*x* enzyme and enhance the efficiency of electrical communication. It is reported that nanoparticles can promote electron transfer between electrodes and the active center of GO*x*, based on the advantageous properties of nanoparticles such as high surface reactivity, high catalytic efficiency and strong adsorption ability for the immobilization of the desired biosensing molecules [12]. Recently, researchers have applied the novel physical and chemical properties of these nanomaterials to the fabrication of highly sensitive biosensors. For example, Wang *et al* have developed photoelectrochemical sensing of NADH under visible irradiation by using nanoporous TiO_2 [13]. Our previous study showed the fabrication of a highly sensitive glucose biosensor based on the photovoltaic effect of ZnO

nanoparticles which can significantly enhance the response current of a glucose biosensor [14].

Gold nanomaterials have superior biomolecule immobilizing properties and have attracted much interest for the development of GO*x* biosensors [15–17]. Most recently, our group reported the successful utilization of gold nanorods (GNRs) to create a highly responsive biosensor [16, 17]. But in these previous studies, gold nanorods have only been used to immobilize the enzymes to improve the electron transfer between the electrode and the substrate molecule. As is well known, GNRs are excellent candidates for photothermal applications owing to their strongly enhanced absorption and scattering induced by the coherent collective oscillation of electrons at their surface [18]. However, there has still been no attempt to exploit the photothermal properties of GNRs for a GO*x* biosensor.

In this paper we describe the fabrication, characterization and analytical performance of a glucose biosensor based on GNR nanoparticles. Moreover, we investigate the photothermal effect of GNRs on a glucose biosensor in a photocontrolled electrochemical system for the first time. Our experiments show that GNRs can significantly enhance the sensitivity of a GO*x* enzyme electrode due to the electron transfer and photothermal effect of the GNRs. In this system, GNRs can convert light energy to environmental heat which can facilitate the enzyme reaction and speed up electron transfer between the electrode and the substrate molecule. Therefore, this method of fabricating a glucose biosensor by using GNRs not only provides a possible strategy to detect glucose easily and sensitively, but also shows the potential for developing a new generation of highly sensitive photocontrolled biosensors.

2. Materials and methods

2.1. Materials

2.1.1. Chemicals and reagents. GO*x* was obtained from *Aspergillus niger* (Sigma Company, 118 U mg^{-1}). β-D-glucose and cetyltrimethylammonium bromide (CTAB) were purchased from Sigma. L(+)-ascorbic acid (99%), silver nitrate ($AgNO_3$), chlorauric acid ($HAuCl_4{\cdot}3H_2O$), sodium borohydride ($NaBH_4$) and cellulose acetate (CA) were the products of Beijing Shiji Company. All the chemicals were used without further purification. All solutions were prepared with deionized water.

2.2. Preparation of GNRs

As described by Murphy *et al* [19], GNRs were prepared by a seed-mediated growth approach.

2.2.1. Preparation of gold seeds. A 10 ml aqueous solution containing 9×10^{-2} M CTAB and 3×10^{-4} M trisodium citrate was mixed in a conical flask in an ice water bath. Then, 0.7 ml of 0.1 M ice-cooled $NaBH_4$ was added to the solution while stirring. The solution turned brownish yellow immediately after adding $NaBH_4$, indicating formation of the gold seed solution.

2.2.2. Preparation of GNRs. First, 0.15 ml of 4×10^{-3} M $AgNO_3$ was added to 10 ml of 9.5×10^{-2} M CTAB solution. Then, 0.1 ml of 4.2×10^{-2} M $HAuCl_4$ was added. After 10 min of gentle shaking, 30 μl of 0.1 M ascorbic acid was added and mixed. Then, 100 μl as-prepared gold seed solution was added to the growth solution. A visual color change from orange-red to purple or blue indicated the formation of GNRs. The temperature of the growth medium was kept constant at 25 °C in all the experiments. The resulting precipitate was centrifuged and washed three times with deionized water.

2.3. Preparation of enzyme electrodes

Pt electrodes with a diameter of 1 mm were cleaned with boiling nitric acid for 5 min and washed with deionized water. Then, 10 μl of 1 U aqueous solution of GO*x* was added to 400 μl of 0.1 mg ml^{-1} GNR solution to form a mixture in a 5 ml beaker. 2 ml of PVB 2-propanol solution (2 wt%) used as an auxiliary membrane matrix and 100 μl glutaraldehyde aqueous solution (1 wt%) used as a crosslinking agent were added to the beaker successively. The contents were stirred evenly by the Pt electrode. Then the Pt electrode was dipped in to a depth of 2 cm for 10 min and taken out. Then the enzyme electrodes were dried in air. A thin membrane was formed on the electrodes. These electrodes were stored at 4 °C for 24 h before any measurement. The enzyme electrodes without GNRs, used as reference samples, were prepared by dipping Pt wire into the mixture containing GO*x*, PVB and glutaraldehyde, the process and amount being the same as described above.

2.4. Characterization

The morphology of the GNRs was visualized by a transmission electron microscope (TEM, JEOL-200CX), operating at 160 kV. All UV–visible–NIR spectra were recorded at room temperature on a JASCO (Japan) V-570 UV–visible–NIR spectrometer using quartz cuvettes with an optical path of 1 cm. A CHI604B electrochemical workstation (Shanghai Chenhua Apparatus Corporation, China) was used for cyclic voltammetric experiments. All experiments were carried out in a three-electrode cell equipped with a modified Pt wire as a working electrode, a Pt wire counter electrode and a Ag/AgCl reference electrode. The applied scan rate was 50 mV s^{-1}.

2.5. Amperometric measurements of the glucose sensor

Amperometric measurements were carried out using a three-electrode cell consisting of an enzyme working electrode, a counter electrode of Pt wire and a reference electrode of Ag/AgCl. Measurements were conducted in a 5 ml phosphate buffer (KH_2PO_4–Na_2HPO_4, pH = 6.8) cell under a fixed potential of 0.4 V at 25 °C. First, the working electrode and reference electrode were put into a phosphate buffer solution. As background current reached a constant value, the response currents were noted down, and then the background currents were deducted. Then, the correlation between the current response and the concentrations of glucose solution was obtained.

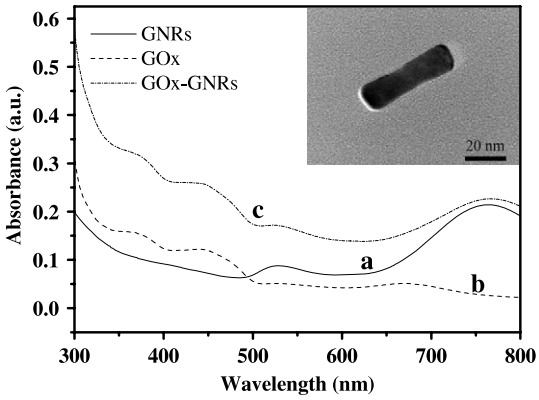

Figure 1. Absorption spectra of (a) GNRs, (b) GO*x*, and (c) GO*x*–GNR bioconjuate. The inset figure is a TEM image of GNRs synthesized by the seed growth method (aspect ratio = 3.5).

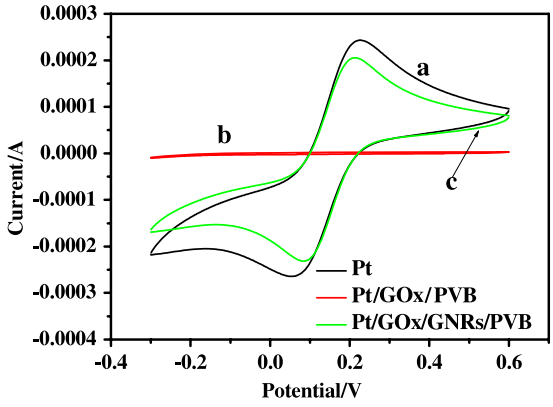

Figure 2. Cyclic voltammograms of 5 mM Fe $(CN)_6^{3-}$ in 0.1 M KCl solution on different modified electrodes at a scan rate of 50 mV s^{-1}: (a) bare Pt, (b) Pt/GO*x*/PVB, and (c) Pt/GOx/GNRs/PVB.

The surface of the modified electrode was irradiated with NIR laser light for 2 min by facing the surface towards a NIR laser light at a distance of 2 cm.

2.6. The temperature elevation experiments with GNR solution

In the temperature elevation experiments, 1 ml of 0.1 mg ml^{-1} GNRs in PBS buffer (phosphate buffered saline, 100 mM Na_2HPO_4/150 mM NaCl, pH 7.4) were exposed to an 808 nm diode laser with a power density of 1 W cm^{-2} (5 W, 20 mm fiber optic patch cable to a collimating lens; Daheng New Epoch Technology, Inc., Beijing, China) for 10 min. The temperature of the solution was detected each minute with the PT-3S thermo-detector made by Optex Co., Ltd, Japan.

3. Results and discussion

3.1. Preparation and optical properties of GNRs

The surface plasmon resonance (SPR) for GNRs is known to split into two bands. The high energy band is induced by the oscillation of the electron perpendicular to the rod axis (transverse surface plasmon absorption). The other absorption band, which is red-shifted to lower energies, is caused by the oscillation of electrons along the rod axis (longitudinal surface plasmon absorption) [20]. Here, in order to obtain SPR of GNRs in the near-infrared (NIR) region (an optical transparency window, where biological tissue and water absorb minimally) so as to avoid GO*x* damage under low laser density, GNRs with an aspect ratio of 3.5 were particularly synthesized to modify the electrodes. The inset of figure 1 shows GNRs prepared via the seed-mediated method as mentioned in section 2.2. The average width of as-prepared GNRs is 15 nm and the average length is 53 nm. Figure 1 shows the absorption spectra of GO*x*, GNRs and GO*x*–GNR aqueous solution. The transverse surface plasmon absorption of GNRs was excited at 520 nm and the longitudinal one at 762 nm (curve a). The absorption peak of pure GO*x* lies at 374 and 450 nm (curve b), consistent with the previous report [21]. After the conjugation of GO*x* with GNRs (curve c), the peaks are slightly shifted to 372, 445 and 767 nm; these shifts may be attributed to the dielectric environment changing after GO*x* absorption on GNRs [18].

3.2. Electrochemical behavior of Pt/GOx/PVB electrode with or without GNRs

Cyclic voltammetry (CV) of an electroactive species is a valuable tool for testing the kinetic barrier of the interface [22]. In this investigation, ferricyanide is used as a mediator for the GO*x* catalyzing the oxidation of glucose. The cyclic voltammograms of different modified electrodes in 5.0 mM ferricyanide solution are shown in figure 2. The bare Pt electrode is characterized by a couple of well-defined redox peaks with anodic and cathodic peak potentials of 220 and 50 mV caused by the Fe^{3+}/Fe^{2+} redox couples (curve a). When the bare Pt electrode was modified by PVB, no obvious redox peaks were noticed due to the insulation properties of the PVB membrane which blocked the electron transfer between the solution and the bare Pt electrode (curve b). After the GNRs were embedded in the PVB membrane, the cyclic voltammetric wave exhibited good symmetry and the current response of CVs greatly increased (curve c), indicating that the electron transfer process is faster at the surface of the composite membrane matrix containing GNRs.

3.3. The current response of the glucose biosensor

To study the effect of GNRs on the sensitivity of the GO*x* biosensor, enzyme electrodes containing GNRs were tested by amperometric measurements. Figure 3 showed the comparison of the current responses of the GO*x* electrode with or without GNRs in the presence of different concentrations of glucose. With increasing glucose concentration, the amperometric response increased. When the GO*x* concentration is 22 mM, the current response of the Pt/GO*x*/PVB electrode is 3.6 μA cm^{-2}. In contrast, that of an electrode with GNRs is 15.5 μA cm^{-2}. This suggests that GNRs can greatly enhance the current response of the modified electrode. This is also consistent with the CV measurement that GNRs can provide a conductive path from GO*x* to the Pt electrode, thus

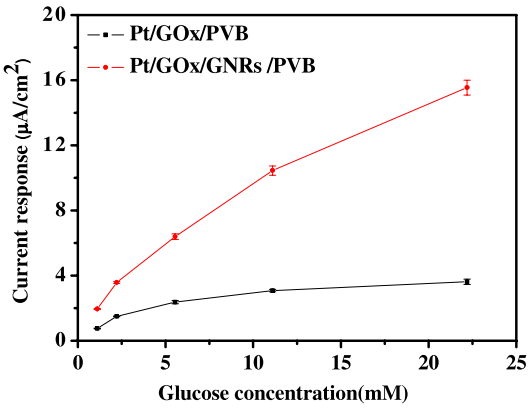

Figure 3. Comparison of the current response of a Pt/GO*x*/PVB electrode with or without GNRs in the presence of different concentrations of glucose (error bars represent the standard deviations of three independent experiments).

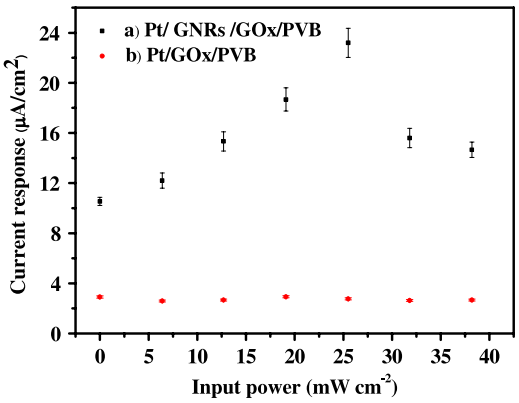

Figure 4. The changes in the current response of a GO*x* electrode (a) with GNRs and (b) without GNRs irradiated by a NIR laser under different power densities (error bars represent standard deviations of five independent experiments).

accelerating the electron transfer rate between GO*x* and the Pt wire and improving the current response significantly.

3.4. The current response of the glucose biosensor under NIR light irradiation

The unique optical properties of GNRs have attracted much interest for their applications in imaging [23], sensing [24], photothermal therapy [18] and so on. Here, our further study reveals an interesting result that the current response of the GNR-modified enzyme electrode can obviously increase under NIR light irradiation compared to a non-modified one. Figure 4 illustrates the change in current response of an enzyme electrode with or without GNRs under 808 nm laser illumination with different laser power densities. All experiments were carried out in 10 mM glucose solution. As figure 4 shows, the average current response of a GNR-modified enzyme electrode without NIR irradiation is 10.5 μA cm^{-2}. With the increase in laser power density, the current response of the GNR-modified enzyme electrode is enhanced. When the laser power density reaches 25.5 mW cm^{-2}, the current response of the GNR-modified enzyme electrode is 23.2 μA cm^{-2}, which is more than twice the initial current response of a GNR-modified enzyme electrode without NIR irradiation. It was found that the current response of the modified biosensor reached a maximum when the laser energy was around 25.5 mW cm^{-2}. When higher laser energy was used, the current response declined. In contrast, the current response of a GO*x* electrode without GNRs during the laser irradiation is also shown in figure 4. The average current response is about 3 μA cm^{-2}, and no obvious regularity was observed.

3.5. Possible mechanism of the electron transfer and photothermal effect of gold nanorods on a glucose biosensor

Regarding the mechanism of electron transfer of a GO*x* modified electrode, our previous research had reported that the nanoparticle surface facilitates immobilization of the enzyme, and improves the activity and stability of the enzyme as a

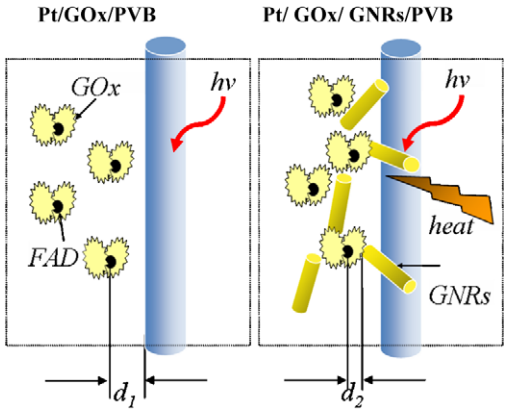

Scheme 1. Schematic representation of a Pt/GO*x*/PVB electrode with or without GNRs under NIR light irradiation. d_1 is the distance between FAD and the metal electrode surface; d_2 is the distance between FAD and the GNRs. The dashed line box denotes the PVB membrane where GO*x* and GNRs are embedded.

result of its higher electroactive surface area, enhanced electron transfer, efficient enzyme immobilization [6, 7, 14, 16, 17]. As is well known, GO*x* is a globular glycoprotein comprising two reaction centers, and each has a flavin adenine dinucleotide (FAD/FADH$_2$) cofactor [25]. In the unmodified Pt electrode, the redox center (FAD/FADH$_2$) of GO*x* is trapped deep in the enzyme, making the distance between FAD and the electrode surface greater than the distance that electrons can transfer sufficiently quickly. For example, in a protein molecule, when the distance between the acceptor and donor increases from 8 to 17 Å, the transfer rate will decrease 10^4 times [1]. With the GNRs deposited on the electrode surface, the distances between FAD and GNRs (d_2) are shorter than the distances between FAD and the electrode (d_1) as shown in scheme 1. GNRs are likely to act as three-dimensional 'electrical wires' to relay electrons from the active center of the enzyme to the surface of the electrode.

Regarding the effect of the NIR light on the GO*x* biosensor, it is not very clear how the NIR laser interacts with the GNRs and further affects the current response of the GO*x*

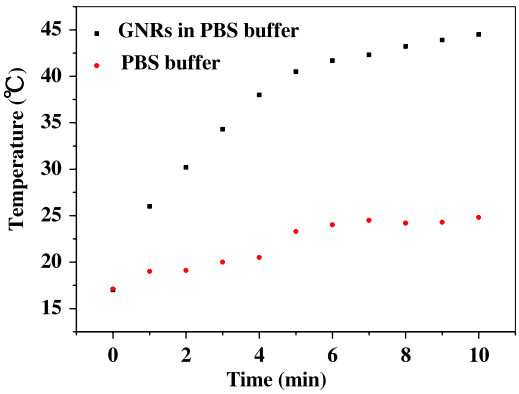

Figure 5. Dependence of the temperature increase of 1 ml 0.1 mg ml^{-1} GNRs PBS buffer on irradiation time.

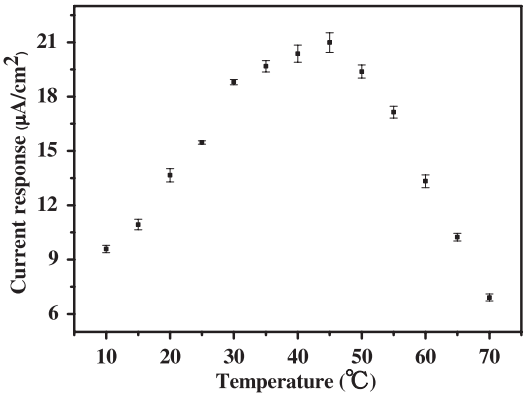

Figure 6. Thermal stability of the GO*x* sensor modified with GNRs (error bars represent standard deviations of three independent experiments).

biosensor. A preliminary explanation could be as follows. After NIR light irradiation, the electromagnetic radiation of the GNRs was strongly enhanced. The embedded GNRs can be modeled as point absorbers, absorbing photon energy, then converting it to thermal energy and dissipating it into the surrounding medium [26]. This thermal dissipation may affect the activity of GO*x* and further affect the current response of the GO*x* biosensor.

To obtain a better insight into the effect of accumulative heating on GO*x* activity, we evaluated the laser light-energy–heat-energy transition efficiency of GNRs and the thermal stability of the GNR-modified GO*x* electrode. The temperature elevation experiments with GNR solution was done under NIR irradiation. The temperature increased with increasing irradiation time. At less than 10 min, the temperature could increase over 30 °C with a power density of 1 W cm^{-2}. In contrast, the temperature of PBS buffer without nanoparticles could only increase less than 10 °C (see figure 5). This result proves that the embedded GNRs can act as nanoscale absorbers of the laser energy and transfer their energy to the environment.

To investigate the thermal stability of the GNR-modified GO*x* electrode, the modified electrode was immersed in buffer solution at different temperatures for 10 min and the steady state currents were recorded. Figure 6 illustrates that the current first increased with increasing temperature, up to a maximum value at about 45 °C, then decreased rapidly to a low value. This current decrease suggests that the transition state of the enzymatic reaction was unstable beyond 45 °C due to enzyme unfolding and denaturation. This current trend is consistent with figure 4, suggesting possible enzyme activity changes as the membrane temperature changes due to the GNR plasmon excitation. In the initial phase, enzyme activity was evaluated with the increase of NIR light laser energy. Moreover, the electrical potential current, redox potential and heterogeneous electron transfer may also be enhanced due to the rise in interfacial temperature [27], and then influence the current response of the modified GO*x* electrode. In the second phase, the current response declined when the laser energy further increased beyond 25.5 mW cm^{-2}. This result may be partly due to denaturing of the GO*x* enzyme when overheated, as shown in figure 6. On the other hand, at high laser power density the melting of GNRs which were no longer resonant at NIR frequencies may also greatly influence the current response [28].

4. Conclusion

We have demonstrated a simple and effective method for the fabrication of highly sensitive glucose biosensor based on gold nanorods, and have revealed for the first time the modulation of a biosensor by the photothermal effect based on the surface plasma resonance of GNRs. The experimental results indicate that the enzyme electrode containing GNRs significantly enhanced the response current compared with electrodes without GNRs. Moreover, it has been proved that the photothermal effect of GNRs can modulate the activity of GO*x* and then improve the performance of the enzyme electrode. In conclusion, this method provides a new feasible way to further enhance and tune the current response of a biosensor using the electron transfer and the photothermal effect of NIR light-absorbing novel metal nanoparticles. We believe this photocontrolled system can be also extended to other amperometric biosensor systems.

Acknowledgments

The authors acknowledge financial support from the National Hi-Tech. Research and Development Program (863 Program) of China (no. 2009AA03z322, and 2007AA021802, 2007AA021804) and the National Natural Science Foundation of China (nos 30800258, 60736001, 20873171)

References

[1] Xiao Y, Patolsky F, Katz E, Hainfeld J F and Willner I 2003 'Plugging into enzymes': nanowiring of redox enzymes by a gold nanoparticle *Science* **299** 1877–81

[2] Reach G and Wilson G S 1992 Can continuous glucose monitoring be used for the treatment of diabetes? *Anal. Chem.* **64** 381A

[3] Gangadharan R, Anandan V and Zhang G 2008 Optimizing the functionalization process for nanopillar enhanced electrodes with GO*x*/PPY for glucose detection *Nanotechnology* **19** 395501

[4] Yuan J P, Guo W W and Wang E K 2008 Quantum dots–bienzyme hybridsystem for the sensitive determination of glucose *Biosens. Bioelectron.* **23** 1567–71

[5] Zhou H, Gan X, Wang J, Zhu X L and Li G X 2005 Hemoglobin based hydrogen peroxide biosensor tuned by the photovoltaic effect of nano titanium dioxide *Anal. Chem.* **77** 6102–4

[6] Ren X L, Meng X W, Chen D, Tang F Q and Jiao J 2005 Using silver nanoparticle to enhance current response of biosensor *Biosen. Bioelectron.* **21** 433–7

[7] Ren X L, Meng X W and Tang F Q 2005 Preparation of Ag–Au nanoparticle and its application to glucose biosensor *Sensors Actuators* B **110** 358–63

[8] Ye J S, Ottova A, Tien H T and Sheu F S 2003 Nanostructured platinum–lipid bilayer composite as biosensor *Bioelectrochemistry* **59** 65–72

[9] Gill R, Bahshi L, Freeman R and Willner I 2008 Optical detection of glucose and acetylcholine esterase inhibitors by H_2O_2-sensitive CdSe/ZnS quantum dots *Angew. Chem. Int. Edn* **47** 1676–9

[10] Serra A, Filippo E, Re M, Palmisano M, Vittori-Antisari M, Buccolieri A and Manno D 2009 Non-functionalized silver nanoparticles for a localized surface plasmon resonance-based glucose sensor *Nanotechnology* **20** 165501

[11] Xie J N, Wang S Y, Aryasomayajula L and Varadan V K 2007 Platinum decorated carbon nanotubes for highly sensitive amperometric glucose sensing *Nanotechnology* **18** 065503

[12] Dai M Q, Gou L and Ran J G 2008 Effect of surface charges of nanoparticles on response current of enzyme electrode for single use *Sensors Actuators* B **113** 565–70

[13] Wang G L, Xu J J and Chen H Y 2009 Dopamine sensitized nanoporous TiO_2 film on electrodes: photoelectrochemical sensing of NADH under visible irradiation *Biosens. Bioelectron.* **24** 2494–8

[14] Ren X L, Chen D, Meng X W, Tang F Q, Hou X Q, Han D and Zhang L 2009 Zinc oxide nanoparticles/glucose oxidase photoelectrochemical system for the fabrication of biosensor *J. Colloid Interface Sci.* **334** 183–7

[15] Xu Q, Mao C, Liu N N, Zhu J J and Sheng J 2006 Direct electrochemistry of horseradish peroxidase based on biocompatible carboxymethyl chitosan-gold nanoparticle nanocomposite *Biosens. Bioelectron.* **22** 768–73

[16] Ren X L, Chen D, Meng X W, Tang F Q, Du A M and Zhang L 2009 Amperometric glucose biosensor based on a gold nanorods/cellulose acetate composite film as immobilization matrix *Colloids Surf.* B **72** 188–92

[17] Ren X L, Tang F Q, Liao R and Zhang L 2009 Using gold nanorods to enhance the current response of a choline biosensor *Electrochim. Acta* **54** 7248–53

[18] Kelly K L, Coronado E, Zhao L L and Schatz G C 2003 The optical properties of metal nanoparticles: the influence of size, shape, and dielectric environment *J. Phys. Chem.* B **107** 668–77

[19] Murphy C J, Sau T K, Gole A M, Orendorff C J, Gao J X, Gou L F, Hunyadi S E and Li T J 2005 Anisotropic metal nanoparticles: synthesis, assembly, and optical applications *J. Phys. Chem.* B **109** 13857–70

[20] Link S and El-sayed M A 2000 Shape and size dependence of radiative, non-radiative and photothermal properties of gold nanocrystals *Int. Rev. Phys. Chem.* **19** 409–53

[21] Chi Q J, Zhang J D, Dong S J and Wang E K 1994 Direct observation of native and unfolded glucose oxidase structures by scanning tunneling microscopy *J. Chem. Soc. Faraday Trans.* **90** 2057–60

[22] Jia J, Wang B, Wu A, Cheng G, Li Z and Dong S 2002 A method to construct a third-generation horseradish peroxidase biosensor: self-assembling gold nanoparticles to three-dimensional sol-gel network *Anal. Chem.* **74** 2217–23

[23] Wang H F, Huff T B, Zweifel D A, He W, Low P S, Wei A and Cheng J X 2005 *In vitro* and *in vivo* two-photon luminescence imaging of single gold nanorods *Proc. Natl Acad. Sci.* **102** 15752–6

[24] Sönnichsen C and Alivisatos A P 2005 Gold nanorods as novel nonbleaching plasmon-based orientation sensors for polarized single-particle microscopy *Nano Lett.* **5** 301–4

[25] Wang J 2008 Electrochemical glucose biosensors *Chem. Rev.* **108** 814–25

[26] Zijlstra P, Chon J and Gu M 2007 Effect of heat accumulation on the dynamic range of a gold nanorod doped polymer nanocomposite for optical laser writing and patterning *Opt. Express* **15** 12151–60

[27] Grant M and Jordan R B 1981 Kinetics of solvent water exchange on iron(III) *Inorg. Chem.* **20** 55–60

[28] Link S and El-Sayed M A 2001 Spectroscopic determination of the melting energy of a gold nanorod *J. Chem. Phys.* **114** 2362–8